Introduction of Dark Matter: Exercise [Ver.2]

Motoko Fujiwara,[*] Martin Wolf[†]

Physik-Department, Technische Universität, München,

James-Franck-Straße, 85748 Garching, Germany

May 12, 2023

This is an exercise for the course of "Applied Multi-Messenger Astronomy 2."

1 Dark Matter (DM) density profile

(1) Plot the Navarro-Frenk-White (NFW) profile density as function of r (distance from the galactic center) by using `python`. The NFW profile is defined below as function of the distance from the galactic center, r.

$$\rho_{\text{NFW}}(r) \equiv \rho_s \left(\frac{r}{r_s}\right)^{-1} \left(1 + \frac{r}{r_s}\right)^{-2}, \tag{1}$$

where

$$r_s = 24.42 \text{ kpc}, \tag{2}$$

$$\rho_s = 0.184 \text{ GeV cm}^{-3}. \tag{3}$$

Hint: In the center part of the galaxy, there is a black hole. To focus on the DM density that can contribute to the experimental/observational signatures, we should get rid of the region that is characterized by the Schwarzschild radius of the black hole (BH) [1].

$$\rho_\chi(r) = \begin{cases} 0 & (r \leq 2R_{\text{sch}}) \\ \rho_{\text{NFW}}(r) & (2R_{\text{sch}} < r \leq R_{\text{vir}}) \end{cases}. \tag{4}$$

This classification is crucial to avoid the singularity in ρ_{NFW} at $r = 0$. We can use the following numerical values for the plot.

$$c = 299792458 \text{ m/s}, \qquad : \text{Speed of light} \tag{5}$$

$$G = 6.67430(15) \times 10^{-11} \text{ m}^3 \text{ kg}^{-1} \text{ s}^{-2}, \quad : \text{Gravitational constant} \tag{6}$$

$$M_{\text{BH}} = 4.154(14) \times 10^6 \ M_\odot, \qquad : \text{Mass of BH (for SgrA}^*) \tag{7}$$

$$r_\odot \simeq 8.4 \text{ kpc}, \qquad : \text{Distance from galactic center} \tag{8}$$

$$R_{\text{sch}} = \frac{2GM_{\text{BH}}}{c^2} = 3.975 \times 10^{-10} \text{ kpc}, \qquad : \text{Schwarzschild radius of BH} \tag{9}$$

$$R_{\text{vir}} = 200 \text{ kpc}. \qquad : \text{Halo's virial radius} \tag{10}$$

Answer: See the blue curve in Fig. 2.

---

[*]E-mail address: `motoko.fujiwara@tum.de`
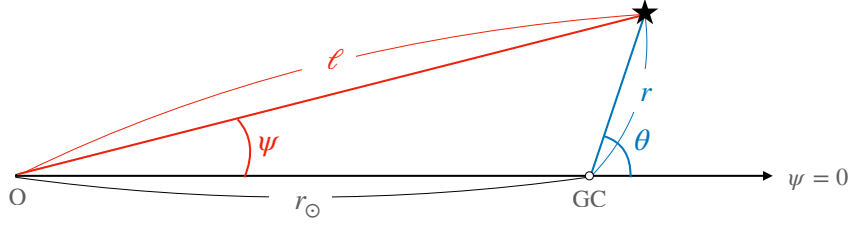
[†]E-mail address: `martin.wolf@tum.de`

Figure 1: The spherical coordinate (blue) vs the line-of-sight coordinate (red). GC and O correspond to the galactic center and the observer's eye, respectively.

(2) It is convenient to change the spherical coordinate (r, θ) into the line-of-sight coordinate (ℓ, ψ) to evaluate DM flux.[1]

(a) Express r and $\cos\theta$ as functions of (ℓ, ψ).
Answer:

$$r = \sqrt{\ell^2 - 2\ell r_\odot \cos\psi + r_\odot^2},$$
$$\cos\theta = \frac{\ell\cos\psi - r_\odot}{r}.$$

(b) Derive Jacobian of this coordinate transformation.
Answer:

$$(\text{Jacobian}) = -\frac{\ell^2}{r^2}\sin\psi.$$

Solution: It is convenient to perform the coordinate transformation from $(r, \cos\theta, \varphi)$ to (ℓ, ψ, φ).

$$dV = r^2\sin\theta\, dr\, d\theta\, d\varphi$$
$$= r^2 dr\, d\cos\theta\, d\varphi.$$

The Jacobian is derived as follow.

$$(\text{Jacobian}) \equiv \begin{vmatrix} \frac{\partial r}{\partial \ell} & \frac{\partial r}{\partial \psi} & \frac{\partial r}{\partial \varphi} \\ \frac{\partial \cos\theta}{\partial \ell} & \frac{\partial \cos\theta}{\partial \psi} & \frac{\partial \cos\theta}{\partial \varphi} \\ \frac{\partial \varphi}{\partial \ell} & \frac{\partial \varphi}{\partial \psi} & \frac{\partial \varphi}{\partial \varphi} \end{vmatrix}$$

$$= \begin{vmatrix} \frac{\ell - r_\odot}{r} & \frac{r_\odot \ell \sin\psi}{r} & 0 \\ \frac{r_\odot \ell \sin^2\psi}{r^3} & \frac{\ell^2 \sin\psi(r_\odot\cos\psi - \ell)}{r^3} & 0 \\ 0 & 0 & 1 \end{vmatrix}$$

$$= -\frac{\ell^2}{r^2}\sin\psi.$$

---

[1]Note that DM density profile is symmetric around the rotational axis of the galaxy. We can fix the azimuth angle φ to be an arbitrary value and focus on (r, θ) in the spherical coordinate or (ℓ, ψ) in the line-of-sight coordinate.

(c) Express the volume element for the line-of-sight integral.

Answer:

$$dV = \ell^2 \sin \psi d\ell d\psi d\varphi.$$

In the end, we should just rename the name of coordinate $(r, \theta) \to (\ell, \psi)$. This is because we only shift the origin to measure distance and angle.

- Spherical coordinate: the galactic center (point GC of Fig. 1)
- Line-of-sight coordinate: the observer's eye (point O of Fig. 1)

Note that the integral region should be changed in the correct manner (cf. exercise 2-(2)).

Solution:

$$\begin{aligned} dV &= r^2 dr d\cos\theta d\varphi \\ &= r^2 \cdot \left(\frac{\ell^2}{r^2} \sin\psi\right) \cdot dr d\cos\theta d\varphi \\ &= \ell^2 \sin\psi d\ell d\psi d\varphi. \end{aligned}$$

(3) Define the NFW profile density as a function of (ℓ, ψ) and reproduce the same plot in exercise (1) by using `python`.

Hint:

- To compare with the density profile in the spherical coordinate, we can plot the density profile in line-of-sight coordinate by choosing the following (x, y) data lists.

$$x = r(\ell, \psi), \tag{11}$$
$$y = \rho_\chi(\ell, \psi). \tag{12}$$

- For crosschecking the result, we can fix $\psi = 0$ ($\cos \psi = 1$) where we find

$$r(\ell, \psi = 0) = |\ell - r_\odot|. \tag{13}$$

We can reconstruct the whole DM density profile by plotting $\rho_\chi(\ell, \psi = 0)$ for $r_\odot \leq \ell < R_{\text{vir}} - r_\odot$.
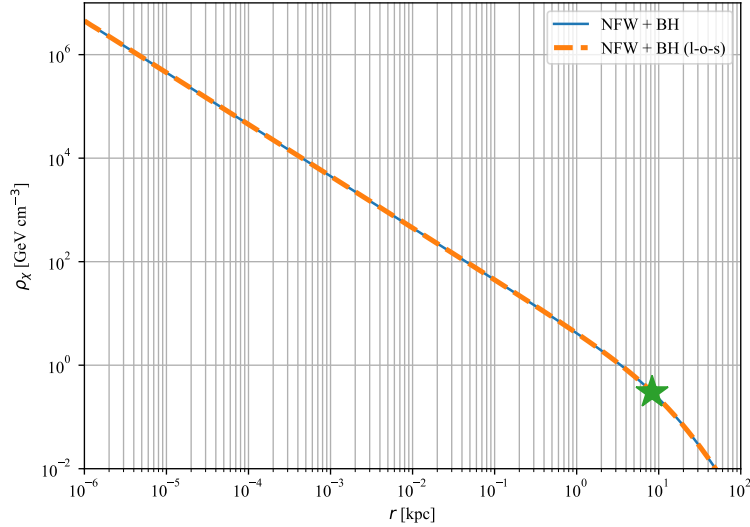
Answer: See Fig. 2.

Figure 2: Plot of DM density profile (NFW+BH). The blue solid curve and the orange dashed curve show the density profile in the spherical coordinate and the line-of-sight coordinate, respectively.

2   *J*-factor and flux

Let us consider the DM pair annihilation into two photons, $\chi\chi \to \gamma\gamma$ (χ: DM, γ: photon). The differential number of gamma-ray photon emitted from volume dV in time interval dt and energy range dE is expressed as follows.

$$dN_\gamma = \frac{dN_\gamma}{dE} \frac{\langle\sigma_{\mathrm{ann}}v\rangle}{2!} \left(\frac{\rho_\chi}{m_\chi}\right)^2 dt\,dE\,dV \frac{dA}{4\pi\ell^2} \tag{14}$$

where we assume that the emission is isotropic and that the anti-particle of DM is DM itself. In this case, the factor of $1/2!$ is necessary to avoid the double-counting of the initial DM particles. We introduce the following variables.

$$\frac{dN_\gamma}{dE} \qquad\qquad \text{: Energy spectrum of gamma-ray photon} \tag{15}$$

$$\langle\sigma_{\mathrm{ann}}v\rangle \qquad\qquad \text{: Velocity-weighted annihilation cross section for DM} \tag{16}$$

$$dA \qquad\qquad \text{: Effective area of the detector} \tag{17}$$

$$\ell \qquad\qquad \text{: Line of sight distance from the observer} \tag{18}$$

$$\tag{19}$$

The energy spectrum from DM annihilation is expressed below:[2]

$$\frac{d\Phi_\gamma}{dE} \equiv \frac{dN_\gamma}{dt\,dE\,dA} = \frac{1}{4\pi} \frac{\langle\sigma_{\mathrm{ann}}v\rangle}{2!m_\chi^2} \frac{dN_\gamma}{dE} \int \frac{\rho_\chi^2(r)}{\ell^2} dV \tag{20}$$

(1) Using the result of exercise 1-(2) and expressing the integral in the line-of-sight coordinate, verify the following energy flux formula.

$$\frac{d\Phi_\gamma}{dE} = \frac{r_\odot}{4\pi} \frac{\langle\sigma_{\mathrm{ann}}v\rangle}{2!} \left(\frac{\rho_\odot}{m_\chi}\right)^2 \frac{dN_\gamma}{dE} \times J, \tag{21}$$

where $\rho_\odot$ is given below.

$$\rho_\chi = 0.3 \text{ GeV cm}^3 \qquad \text{: local DM density in our solar system} \tag{22}$$

We introduce a dimensionless integral J, called *J*-factor, to characterize flux.

$$J \equiv 2\pi \int_0^\pi d\psi \sin\psi \int_{\mathrm{l.o.s}} \frac{d\ell}{r_\odot} \left(\frac{\rho_\chi}{\rho_\odot}\right)^2, \tag{23}$$

where l.o.s expresses the integral over the gray region in Fig. 3.

Hint: Use the result of exercise 1-(2).

(2) Evaluate *J*-factor in Eq. (23) for the NFW+BH profile derived in exercise 1.
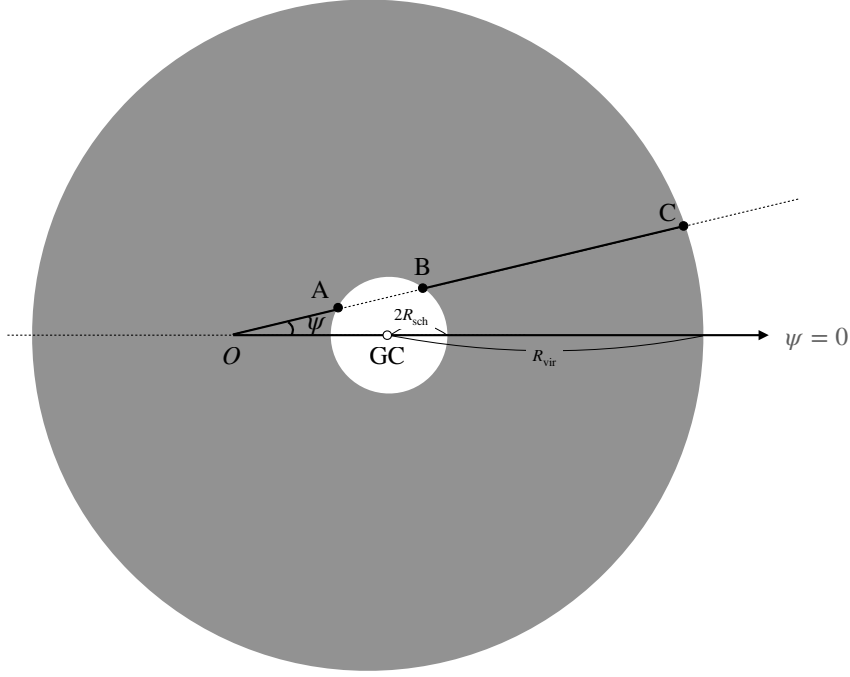
---

[2]See Eq. (1) in Ref. [2].

Figure 3: Integral region of the J-factor.

Hint: If we consider $\psi \leq \sin^{-1}(R_{\text{sch}}/r_\odot)$, the integral region for ℓ can be characterized as the following values of ℓ at $\{A, B, C\}$ in Fig. 3.

$$\ell_A = r_\odot \left(\cos \psi - \sqrt{\left(\frac{2R_{\text{sch}}}{r_\odot} \right)^2 - \sin^2 \psi} \right), \tag{24}$$

$$\ell_B = r_\odot \left(\cos \psi + \sqrt{\left(\frac{2R_{\text{sch}}}{r_\odot} \right)^2 - \sin^2 \psi} \right), \tag{25}$$

$$\ell_C = r_\odot \left(\cos \psi + \sqrt{\left(\frac{R_{\text{vir}}}{r_\odot} \right)^2 - \sin^2 \psi} \right). \tag{26}$$

Since we already get rid of the region in $\ell \in [\ell_A, \ell_B]$ in the definition of ρ_χ, all we have to do is to integrate over $\ell \in [\ell_{\min}, \ell_{\max}]$ where

$$\ell_{\min} = 0, \tag{27}$$
$$\ell_{\max} = \ell_C. \tag{28}$$

The strategy is the same for $\psi > \sin^{-1}(R_{\text{sch}}/r_\odot)$.

Answer:

$$J = 34.6.$$

6

(3) Evaluate photon flux of DM annihilation by assuming that DM annihilation process is dominated by $\chi\chi \to \gamma\gamma$.[3]

Hint: We can use the following benchmark values for the standard WIMP scenario.

$$(\sigma_{\mathrm{ann}}v) = 3 \times 10^{-26} \ \mathrm{cm}^3/s \quad : \text{Annihilation cross section for WIMP scenario} \tag{29}$$

$$m_\chi = 300 \ \mathrm{GeV} \qquad\qquad : \text{DM mass for WIMP scenario} \tag{30}$$

For the annihilation process $\chi\chi \to \gamma\gamma$, we have

$$\frac{dN_\gamma}{dE} = 2\delta(E - m_\chi). \tag{31}$$

Answer:

$$\Phi_\gamma = 2.2 \times 10^{-9} \ \mathrm{cm}^{-2} \ \mathrm{s}^{-1} \left(\frac{(\sigma_{\mathrm{ann}}v)}{3 \times 10^{-26} \ \mathrm{cm}^3/\mathrm{s}} \right) \left(\frac{300 \ \mathrm{GeV}}{m_\chi} \right)^2.$$

3 Spike structure

If the accretion of DM is adiabatic and relativistic effects are neglected, even steeper exponent may appear in the center part, which is called *spike structure*. If we naively implement this spike structure for the NFW profile, we obtain the following profile.

$$\rho_\chi(r) \overset{!}{=} \begin{cases} 0 & (r \le 2R_{\mathrm{sch}}) \\ \rho_{\mathrm{sp}}(r) & (2R_{\mathrm{sch}} < r \le R_{\mathrm{sp}}) \ , \\ \rho_{\mathrm{NFW}}(r) & (R_{\mathrm{sp}} < r \le R_{\mathrm{vir}}) \end{cases} \tag{32}$$

where

$$\rho_{\mathrm{sp}}(r) = \rho_{\mathrm{NFW}}(R_{\mathrm{sp}}) \left(\frac{r}{R_{\mathrm{sp}}} \right)^{-\gamma_{\mathrm{sp}}}, \tag{33}$$

and

$$R_{\mathrm{sp}} \simeq 1 \ \mathrm{pc}, \qquad\qquad : \text{Spike radius (benchmark value)} \tag{34}$$

$$\gamma_{\mathrm{sp}} = \frac{7}{3}. \qquad\qquad : \text{Scaling exponent of spike structure} \tag{35}$$

DM constraints are derived using IceCube results assuming this spike structure [5, 6]. However, in the center part of this spike profile, DM density reaches so high that DM processes (such as DM annihilation and DM decay) may dissolve the profile. Let us take a look at the spike structure and derive the condition for the dissolution.

---

[3]Since DM is electrically neutral, the annihilation channel is suppressed compared to other annihilation channels. However, some DM candidates predict the enhanced annihilation cross section into photons for specific DM mass. This effect is first pointed out in Ref. [3] and now accurately calculated in Ref. [4] (The predicted value of $(\sigma_{\mathrm{ann}}v)$ is shown in Fig. 3).

(1) Discuss what kind of criteria can characterize the condition for DM density dissolution.

Hint:

$$\text{(typical time scale for the DM annihilation)} \simeq \frac{1}{n_\chi \langle \sigma_{\text{ann}} v \rangle} = \frac{m_\chi}{\rho_\chi \langle \sigma_{\text{ann}} v \rangle}, \quad (36)$$

$$\text{(typical time since the spike formation)} \simeq 10 \text{ Gyr}. \quad (37)$$

Answer: If we find

$$\text{(time scale of DM annihilation process)} \lesssim \text{(time since the spike formation)},$$

the DM annihilation process dissolves the density profile.

(2) The time evolution of DM number density is described by the following equation if the DM number changes through the DM pair annihilation.

$$\dot{n}_\chi(r,t) = -(\sigma_{\text{ann}} v) n_\chi(r,t)^2. \quad (38)$$

Derive the analytical solution of this equation by integrating from t_f, the time the spike is formed, to t.

Answer:

$$n_\chi(r,t) = \frac{n_\chi(r,t_f)}{1 + n_\chi(r,t_f)(\sigma_{\text{ann}} v)(t - t_f)}.$$

(3) Derive the upper bound on ρ_χ at given (r,t) and express the DM density profile that is consistent with the upper bound.

Hint: The number density derived in exercise 3-(2) can be applied to the region where the DM annihilation process effectively occurs.[4] In other words, if the DM number density exceed this value, the rate of DM annihilation is so rapid that DM may disappear. In this sense, we can interpret this value as the upper bound on DM number density where the spike structure holds. Since we can safely assume $(t - t_f) \gg 1/(n_\chi(r,t_f)(\sigma_{\text{ann}} v))$, which is the condition for the DM annihilation process to effectively occur at the time of the spike formation (cf. 3-(1)), we can derive the upper bound on the DM mass density, ρ_{pl}.

$$\rho_{pl}(t) \equiv \frac{m_\chi}{(\sigma_{\text{ann}} v)(t - t_f)}$$

$$= 3.2 \times 10^{10} \text{ GeVcm}^{-3} \left(\frac{m_\chi}{300 \text{ GeV}} \right) \left(\frac{3 \times 10^{-26} \text{ cm}^3 \text{s}^{-1}}{(\sigma_{\text{ann}} v)} \right) \left(\frac{10 \text{ Gyr}}{t - t_f} \right).$$

Note that the final result is independent of r, and this value can be applied as the upper bound on ρ_χ for given t everywhere. Therefore, the density will be saturated

---

[4]If we can neglect DM annihilation, the right hand side will be 0, and the density does not evolve in time.

by the dissolution effect due to the DM annihilation in the region where $\rho_\chi(r) > \rho_{\rm pl}$. The density profile is expressed as follows.

$$\rho_\chi(r) = \begin{cases} 0 & (r \leq 2R_{\rm sch}) & : \text{BH region} \\ \rho_{\rm pl} & (2R_{\rm sch} < r \leq R_{\rm pl}) & : \text{plateau region} \\ \rho_{\rm sp}(r) & (R_{\rm pl} < r \leq R_{\rm sp}) & : \text{spike region} \\ \rho_{\rm NFW}(r) & (R_{\rm sp} < r \leq R_{\rm vir}) & : \text{halo(NFW) region} \end{cases},$$

where $R_{\rm pl}$ is defined through the following condition.

$$\rho_{\rm sp}(R_{\rm pl}) = \rho_{\rm pl}(t).$$

Answer: See Fig. 4. In this plot, we take $t - t_f = 10$ Gyr as benchmark.
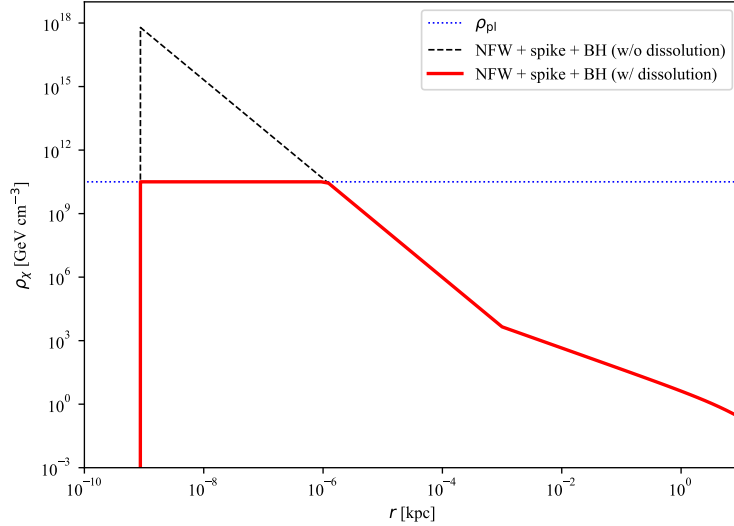

Figure 4: Plot of DM density profile (NFW+spike+BH). The $\rho_{\rm pl}$ is shown as the blue dotted line. The red solid curve and the black dashed curve show the profile with and without the dissolution effect, respectively.

References

[1] L. Sadeghian, F. Ferrer, and C. M. Will, *Dark matter distributions around massive black holes: A general relativistic analysis*, Phys. Rev. D **88** (2013) 063522 [arXiv:1305.2619].

[2] L. Rinchiuso, *et al.*, *Hunting for Heavy Winos in the Galactic Center*, Phys. Rev. D **98** (2018) 123014 [arXiv:1808.04388].

[3] J. Hisano, S. Matsumoto, M. M. Nojiri, and O. Saito, *Non-perturbative effect on dark matter annihilation and gamma ray signature from galactic center*, Phys. Rev. D **71** (2005) 063528 [`hep-ph/0412403`].

[4] M. Beneke, A. Broggio, C. Hasner, K. Urban, and M. Vollmann, *Resummed photon spectrum from dark matter annihilation for intermediate and narrow energy resolution*, JHEP **08** (2019) 103 [`arXiv:1903.08702`]. [Erratum: JHEP 07, 145 (2020)].

[5] F. Ferrer, G. Herrera, and A. Ibarra, *New constraints on the dark matter-neutrino and dark matter-photon scattering cross sections from TXS 0506+056*, `arXiv:2209.06339` (2022).

[6] J. M. Cline and M. Puel, *NGC 1068 constraints on neutrino-dark matter scattering*, `arXiv:2301.08756` (2023).